PCCP

Accepted Manuscript

ROYAL SOCIETY OF CHEMISTRY

www.rsc.org/pccp

Journal Name

RSCPublishing

ARTICLE

Peptides Containing Blocks of Different Charge Densities Facilitate Cell Uptake of Oligonucleotide

-Cite this: DOI: 10.1039/x0xx00000x

Jihan Zhou[‡], Dong Li[‡], Cuicui Su, Hao Wen, Quan Du[*] and Dehai Liang[*]

Received 00th January 2012,
Accepted 00th January 2012

DOI: 10.1039/x0xx00000x

www.rsc.org/

Polyelectrolyte complexes (PECs) are of great importance in drug delivery and gene therapy. The density and the distribution of the charges are key parameters of a polyelectrolyte, determining the structure of the complex and the kinetics of the complexation. Using peptides of precisely-controlled charge density as model molecules, we showed that the presence of weakly-charged peptides, $(KGGG)_5$ or $(KGKG)_5$, did not affect the complexation of highly-charged peptides $(KKKK)_5$ with a 21 bp oligonucleotides. However, peptide containing blocks of different charge density, such as $(KKKK)_5$-*b*-$(KGGG)_5$ or $(KKKK)_5$-*b*-$(KGKG)_5$, exhibited superior performance during complexation. With relatively uniform small size, the complex was also stable in serum. More importantly, cellular uptake of the complex was greatly enhanced by a ratio of 40~60%, compared to that of the complex formed by uniformly-charged peptides. We attributed the improvement to the structure of the complex, in which the highly-charged blocks form the core with the oligonucleotide whilst the weakly-charged blocks dangle outside, preventing the complexes from further aggregation.

Introduction

Gene therapy requires vehicles that are able to deliver DNA or siRNA to the target cells in a safe and efficient manner.[1-5] As the negatively charged DNA/RNA molecules can be condensed and encapsulated by polycations, the complex particle, generally known as polyelectrolyte complex (PEC), has been considered as a potential gene delivery carrier. Both cationic polymers and cationic lipids have been extensively tested as non-viral vectors for siRNA and DNA delivery.[6-13] However, these vectors are still far from clinic applications, mainly due to their low transfection efficiency.

For a given plasmid DNA, the physicochemical properties of the complexes are determined by the intrinsic features of the cationic polymers, such as charge density[14] and topology.[15,16] In addition, the structure and properties of the complexes can be tuned by varying the external conditions,[17-22] including mixing ratio, concentration, ionic strength, pH, solvent quality, and so on. Because the electrostatic interaction is strong and long-ranged, the DNA complex is also controlled by kinetics to a large extent.[23,24] The physicochemical properties of DNA/siRNA complexes, such as size, stiffness, surface charge, stability and morphology, are closely related to the performance in cell transfection. For example, the particles with size smaller than 150 nm were able to pass through the cell membrane via non-clathrin-coated endocytosis,[25,26] while the diffusion and cell uptake were hindered if the size of complex reached 300 nm.[27] Many results suggested that particles with anisotropic symmetry, such as rod, disc or deformable particles displayed enhanced cell uptake.[28,29] Moreover, polycations with branched[30,31] or dendritic[32,33] structure were more active during cell uptake.

Charge density played an essential role in the complex formation. It was generally accepted that the polymers with higher charge density were more effective in condensing and encapsulating DNA.[34,35] Since the cell membrane is negatively charged, the positively charged complex, which was obtained by varying the +/- charge ratio, exhibited enhanced cell internalization compared to the negatively charged complex. However, the positively charged complex was not stable in serum, and was quickly cleared by reticuloendothelial system. To overcome these barriers, polyethylene glycol (PEG) was employed as a protection reagent to significantly increase the circulation time of the complexes.[36] PEG is a neutral polymer. Its attachment to the periphery of the DNA complex screened the effect charge, resulting in a deterioration of cell internalization. The dilemma of PEG has not been fully resolved. Jiang and coworkers have implemented zwitterionic polymers for protein conjugates[37] or peptides with both negatively and positively charged groups for gold nanoparticles[38] to improve stability in a manner like PEGylation .

Peptides provide a novel platform for gene delivery, due to their low immunogenicity and programmability. Further, charge density of a peptides can be precisely-controlled. We therefore speculate that peptides with blocks of different charge densities may achieve selective binding of DNA by the block of higher charge density and effective cell uptake with the help of the block of lower charge density. Furthermore, weakly

charged block may stabilize the complex with electrostatic repulsion to improve stability. To test this hypothesis, five peptides were designed in this study, using only two amino acids, lysine (K) and glycine (G). Sequences of the peptides are listed in Table 1. The charge density of the first three peptides decreased in the order of $(KKKK)_5$, $(KGKG)_5$, and $(KGGG)_5$. Two di-block peptides were obtained by linking a $(KKKK)_5$ block with a $(KGKG)_5$ or $(KGGG)_5$ block. A double-stranded oligonucleotide of 21 bp, whose length was close to that of a peptide of 20 amino acids, was used to test the complexation behavior of the peptides. Cell uptake efficiency of the peptide/DNA complexes was tested in cultured cells, to build a relationship between the physicochemical properties of the complexes and their cell-based activities.

Table 1. Sequences of the peptides

Peptide name	Sequence	δ*
$(KKKK)_5$	Ac-KKKK KKKK KKKK KKKK KKKK-amide	0.95
$(KGKG)_5$	Ac-KGKG KGKG KGKG KGKG KGKG-amide	0.50
$(KGGG)_5$	Ac-KGGG KGGG KGGG KGGG KGGG-amide	0.25
†$(KKKK)_5$-*b*-$(KGKG)_5$	Ac-KKKK KKKK KKKK KKKK KKKK GKGK GKGK GKGK GKGK GKGK-amide	0.73
†$(KKKK)_5$-*b*-$(KGGG)_5$	Ac-KKKK KKKK KKKK KKKK KKKK GGGK GGGK GGGK GGGK GGGK-amide	0.60

K: lysine, G: glycine; *δ: relative charge density = effective charges / number of amino acid groups in the peptide, † The actual sequence of the second block is $(GKGK)_5$ or $(GGGK)_5$.

Experimental

Materials and sample preparation

Peptides (purity >99%) of designed sequence were synthesized by GL Biochem. Ltd. (Shanghai, China). The effective charge of each peptides was calculated by JaMBW 1.1 software (http://www.bioinformatics.org/JaMBW//) (Table S1). The relative charge density δ is defined as the average charge per unit amino acid group of peptide, [39] and the values are listed in Table 1. Oligonucleotides with a random sequence were purchased from Invitrogen (Shanghai, China). Fetal bovine serum was from Macgene (Beijing, China). FITC-labeled oligonucleotides were from RiboBio Co. Ltd. (Guangzhou, China). Trizma® base and EDTA were from Sigma (St Louis, US). Double-stranded oligonucleotide (ds-oligo) was obtained by annealing two complementary single-stranded oligonucleotides at a molar ratio of 1:1 in 1× TE (10 mM tris base, 1 mM EDTA) buffer at 95 °C for 5 min, followed by slow cooling to room temperature. Stock solutions of the peptides and salmon DNA were obtained by dissolving the sample in TE buffer. The resulting solutions were diluted by TE to desired concentrations.

Laser light scattering (LLS)

A commercialized spectrometer from Brookhaven Instruments Corporation (BI-200SM Goniometer, Holtsville, NY) was used to perform both static light scattering (SLS) and dynamic light scattering (DLS) over a scattering angular range of 20-120°. In static light scattering (SLS), the angular dependence of the excess absolute time-averaged scattered intensity, known as the Rayleigh ratio $R_{vv}(\theta)$, was measured. For a very dilute solution, the weight-averaged molar mass (M_w) and the root mean-square radius of gyration (R_g) can be obtained on the basis of

$$HC / R_{vv}(\theta) = (1/M_w)\left[1 + (1/3)R_g^2 q^2\right] + 2A_2 C \quad (1)$$

where $H = 4\pi^2 n^2 (dn/dC)^2/(N_A\lambda^4)$ and $q = 4\pi n/\lambda \sin(\theta/2)$ with N_A, n, dn/dC, and λ being the Avogadro's number, the solvent refractive index, the specific refractive index increment, and the wavelength of light in a vacuum, respectively.

In dynamic light scattering (DLS), the intensity–intensity time correlation function $G^{(2)}(\tau)$ in the self-beating mode was measured

$$G^{(2)}(\tau) = A\left[1 + \beta\left|g^{(1)}(\tau)\right|^2\right] \quad (2)$$

where A is the measured base line, β is a coherence factor, τ is the delay time, and $g^{(1)}(\tau)$ is the normalized first-order electric field time correlation function. $g^{(1)}(\tau)$ is related to the line width distribution $G(\Gamma)$ by

$$g^{(1)}(\tau) = \int_0^\infty G(\Gamma) e^{-\Gamma\tau} d\Gamma \quad (3)$$

By using a Laplace inversion program, CONTIN, the normalized distribution function of the characteristic line width $G(\Gamma)$ was obtained. The average line width, $\overline{\Gamma}$, was calculated according to $\overline{\Gamma} = \int \Gamma G(\Gamma) d\Gamma$. $\overline{\Gamma}$ is a function of both C and q, which can be expressed as

$$\overline{\Gamma}/q^2 = D(1 + k_d C)\left[1 + f(R_g q)^2\right] \quad (4)$$

with D, k_d, f being the translational diffusive coefficient, the diffusion second virial coefficient, and a dimensionless constant, respectively. D can be further converted into the hydrodynamic radius R_h by using the Stokes-Einstein equation:

$$D = k_B T / 6\pi\eta R_h \quad (5)$$

where k_B, T, η are the Boltzmann constant, the absolute temperature, and the viscosity of the solvent, respectively. Detailed LLS description can be found elsewhere.[24]

For LLS measurements, each of the aqueous sample was passed through a 0.20 μm syringe filter (Sartorius stedim Biotech, Goettingen, Germany) to remove the dust. Complexes at different +/- ratios (+/-, a molar charge ratio, obtained by dividing the number of the positive charge on the peptides by the number of negative charge on the DNA molecules) were prepared by mixing peptide and DNA solution together. Each mixture was vortexed for 30 seconds, and then stayed at room temperature for 30 min before measurement.

Atomic force microscopy (AFM)

The images were taken in tapping mode using Nanoscope III equipped with a 110 μm scanner (Veeco. Instrument Inc.). Imaging was performed in air with a FESP tip (Bruker instruments Inc.). The resonant frequency of the cantilever is about 70 kHz. 10 μL of the complex solution was deposited on a fresh mica surface using a pipette. After 30 s, the excess solution was blotted away with a strip of filter paper. The sample was washed with Milli-Q water (Millipore, USA) twice to remove salts. It was then air-dried for one day before AFM measurements.

Zeta potential analysis

Zeta potentials of a complex were measured in TE buffer, using a zeta potential analyzer (Zeta PALS, Brookhaven Iazznstruments, Holtsville, NY) at 25 ^{o}C. The mobility (μ_e) of the complex was determined and the zeta potential ζ was calculated according to Smoluchowski equation $\mu_e = \zeta\varepsilon/\eta$, with ε and η being the dielectric constant and viscosity of the solvent, respectively.

Cell culture and high content analysis

HEK293 cells (an specific cell line originally derived from human embryonic kidney cells) were grown in Dulbecco's modified Eagle's medium supplemented with 10% fetal bovine serum (HyClone Laboratories, Inc.), 100 units/ml penicillin and 100 μg/ml streptomycin (Life Technologies, Gibco). The cells were seeded into 96-well plates at ~6×10^3 cells/well one day before transfection. Peptide/oligonucleotide complexes (+/- = 3.0 or 9.0) were transfected into HEK293 cells at ~50% confluence. Naked oligonucleotide was used as control. The fluorescence was measured by Operetta (PerkinElmer, UK) and the result was analyzed by Columbus system (PerkinElmer, UK).

Results and discussion

Complexation of ds-oligo with mixed peptides

Our previous work demonstrated that $(KKKK)_5$ interacted strongly with ds-oligo to form complexes, and even precipitations at charge ratios close to unity, while the complexation between ds-oligo and $(KGGG)_5$ or $(KGKG)_5$ was fairly weak under the same conditions.[40] To test if peptides of high charge density dominate the complexation with DNA in a mixed system, a high charge density peptide $(KKKK)_5$ was mixed with low charge density peptides $(KGGG)_5$ or $(KGKG)_5$, at a weight ratio of 1:1. Under the same condition, their interactions with a 21bp double-stranded DNA oligonucleotide were comparatively investigated. The complex was prepared by adding a given amount of the oligonucleotide into the $(KKKK)_5$ peptide or its mixtures, in one batch. The +/- charge ratio was calculated assuming that only $(KKKK)_5$ peptides interact with the oligonucleotides. Figure 1 shows the size (hydrodynamic radius, R_h) distribution of the complexes, and their angular dependence of the inversed excess intensity at +/- charge ratio of 3.0. The inversed excess intensity is denoted as $I_t/(I_s\text{-}I_0)$, with I_t, I_s, and I_0 being the scattered intensity from toluene, the complex solution, and the solvent, respectively. It is inversely proportional to the Rayleigh ratio. The size and size distribution of the complex formed by ds-oligo and $(KKKK)_5$ itself (Figure 1A), as well as the scattered intensity(Figure 1B), were almost the same as that in the presence of $(KGGG)_5$ or $(KGKG)_5$. Similar result was obtained at +/- charge ratio of 6.4 (Figure S1). This suggests that $(KGGG)_5$ or $(KGKG)_5$ exhibited negligible effects on the complexation between $(KKKK)_5$ and oligonucleotide. In other words, the oligonucleotide selectively interacted with the peptide of higher charge density at +/- charge ratio larger than unity.

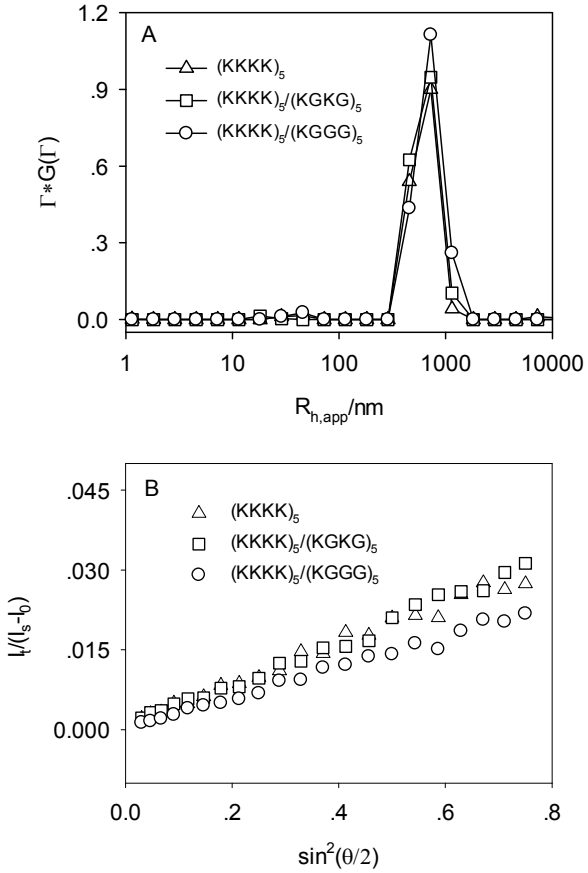

Figure 1. The size distribution (A) and the angular dependence of the inversed excess scattered intensity (B) of the complexes. The complexes were formed by mixing a 21 bp ds-oligo with $(KKKK)_5$ peptide, the mixture of $(KKKK)_5/(KGGG)_5$ or $(KKKK)_5/(KGKG)_5$, at a +/- ratio of 3.0. $c(KKKK)_5 = c(KGGG)_5 = c(KGKG)_5 = 5.0\times10^{-6}$ g/mL, c(oligonucleotide) = 1.0×10^{-5} g/mL.

Complexation of di-block peptides and ds-oligo

Di-block peptides were synthesized by linking the high charge density block $(KKKK)_5$ to the low charge density block, $(KGGG)_5$ or $(KGKG)_5$. According to the established *in vivo* toxicity of cationic materials, minimal cationic components are desirable for DNA or siRNA delivery. Therefore, complexes were prepared by mixing the oligonucleotide with $(KKKK)_5$, $(KKKK)_5$-*b*-$(KGKG)_5$, or $(KKKK)_5$-*b*-$(KGGG)_5$, at a +/- ratio of 3. Distribution of $R_{h,app}$ and the scattered intensity of the complexes were presented in Figure 2. As shown in Figure 2A

and Table 2, the size of the complex formed by single-block peptide $(KKKK)_5$ ($R_{h,app}$, about 340 nm) was much larger than that of the di-block peptide complexes ($R_{h,app}$, ~140 nm). The size distribution was also broader (Figure 2A). The angular dependence of the inversed scattered intensity showed an interesting phenomenon. Even though the scattered intensity after extrapolating to zero angle was similar, the angular dependences of the intensity were different for the three complexes (Figure 2B).

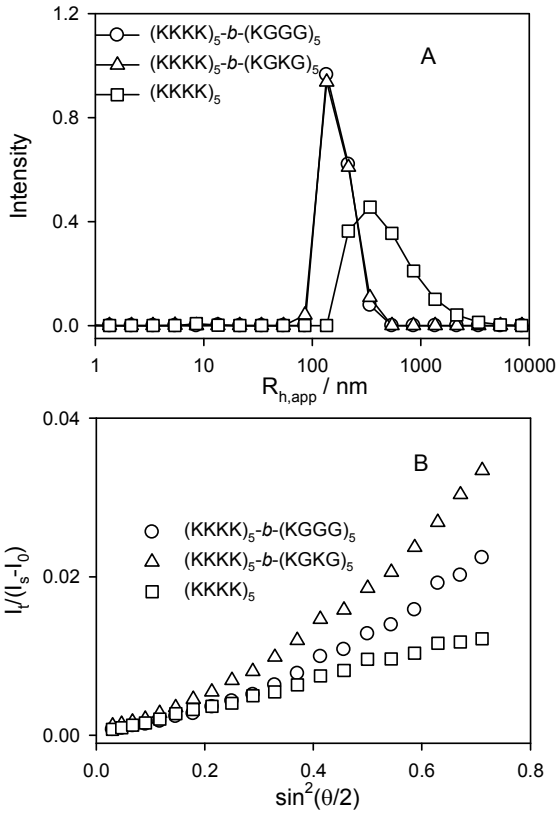

Figure 2. The size distribution at 90°(A) and the angular dependence of the excess scattered intensity (B) of the complexes. The complexes were formed by mixing a 21bp ds-oligo with peptide $(KKKK)_5$, $(KKKK)_5$-*b*-$(KGKG)_5$, or $(KKKK)_5$-*b*-$(KGGG)_5$ at a +/- ratio of 3 in TE buffer. *c*(peptide) =1.0×10^{-5} g/mL, *c*(oligonucleotide) = 1.0×10^{-5} g/mL.

In the scattering vector regime $qR_g > 1$(with q being the scattering vector), the form factor P(q) is given as $\log P(q) = -D_f \log q$.[41] In the $\log P(q)$ vs. $\log q$ plot, the fractal dimension (D_f) of the complexes can be evaluated from the linear decay of the angular dependence. After fitting the curves of Figure 3A, the D_f of the complexes formed by $(KKKK)_5$, $(KKKK)_5$-*b*-$(KGKG)_5$, or $(KKKK)_5$-*b*-$(KGGG)_5$ were 2.1, 3.0 and 3.1, respectively. This result indicated that, compared to the complexes of single-block peptide, the complexes formed by di-block peptide were more dense, and probably with a fractal surface. The form factors of the particles exhibited quite different curves in the Kratky plot (Figure 3B), which can be used to evaluate the branching probability of the complexes.[42,43] Compared to the single-block peptide complexes, the complexes of di-block peptide exhibited a much more negative slope at the asymptotic region, indicating that the complexes adopted a highly-branched conformation.

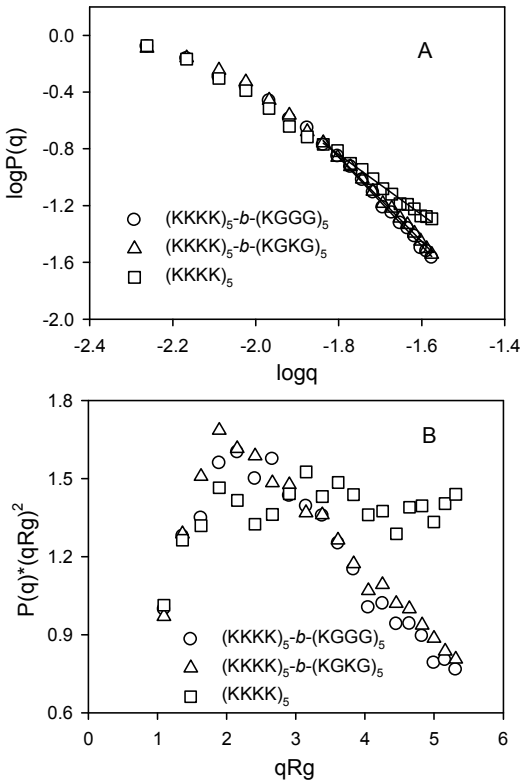

Figure 3. Form factor fitting curves (A) and Kratky plots (B) of the scattered data in Figure 2B.

AFM imaging was performed to characterize the morphology of the complexes. As shown in Figure 4C, complexes formed by oligonucleotide and $(KKKK)_5$ were heavily aggregated and the size of the cluster was much larger. Aggregation of the complexes was alleviated in the case of $(KKKK)_5$-*b*-$(KGKG)_5$. In addition to the spherical complexes, some of the complexes were in tadpole- or dumbbell-shaped (Figure 4B). As for the $(KKKK)_5$-*b*-$(KGGG)_5$, most complexes were of uniform spherical structures, with smaller size and lower height under microscope (Figure 4A). Both the AFM and LLS results indicated that attachment of a weakly-charged block prevented the complex from further aggregating into a large-scaled clusters.

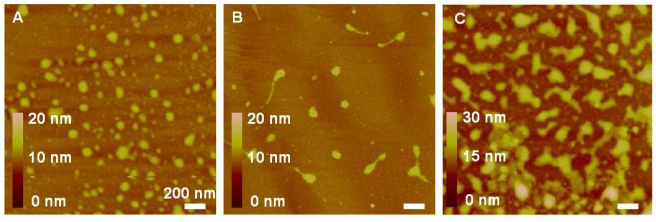

Figure 4. AFM imaging of the complexes formed by a 21 bp oligonucleotide and peptide $(KKKK)_5$-*b*-$(KGGG)_5$ (A), $(KKKK)_5$-*b*-$(KGKG)_5$ (B), and $(KKKK)_5$ (C). The +/- ratio, 3.0; scale bar, 200 nm. *c*(peptide) =1.0×10^{-5} g/mL, *c*(oligonucleotide) = 1.0×10^{-5} g/mL.

To evaluate the surface charge of the complexes, their zeta potentials were measured. All the complexes formed by oligonucleotide and the peptides were slightly positively charged. For complexes of $(KKKK)_5$, $(KKKK)_5$-*b*-$(KGKG)_5$, and $(KKKK)_5$-*b*-$(KGGG)_5$, as shown in Table 2, the zeta potentials were 4.0 ± 2.0, 6.0 ± 2.0, and 8.0 ± 2.0 mV, respectively. These values were calculated by Smoluchowski equation assuming that all the charges were located on the surface of the particle. As DNA complexes were soft particles, the mobility under electric field (from which the zeta potential was calculated) derived not only from the charge density, but also from the softness and the radial charge distributions of the particles.[44,45] It has been reported that swollen ionic microgel migrates faster than the de-swollen microgel due to the solvent free-draining effect, which reduces the friction force during migration.[46] The complex surrounded by less charged peptides showed similar behavior as the swollen ionic microgel. It migrated faster under electric field, and a higher zeta potential was obtained by calculation.

Table 2. Average size and zeta potentials of the complexes

Complex of ds-oligo with	Average size/nm	Zeta potential / mV
$(KKKK)_5$	340	4.0 ± 2.0
$(KKKK)_5$-*b*-$(KGKG)_5$	140	6.0 ± 2.0
$(KKKK)_5$-*b*-$(KGGG)_5$	140	8.0 ± 2.0

Stability of complex in serum

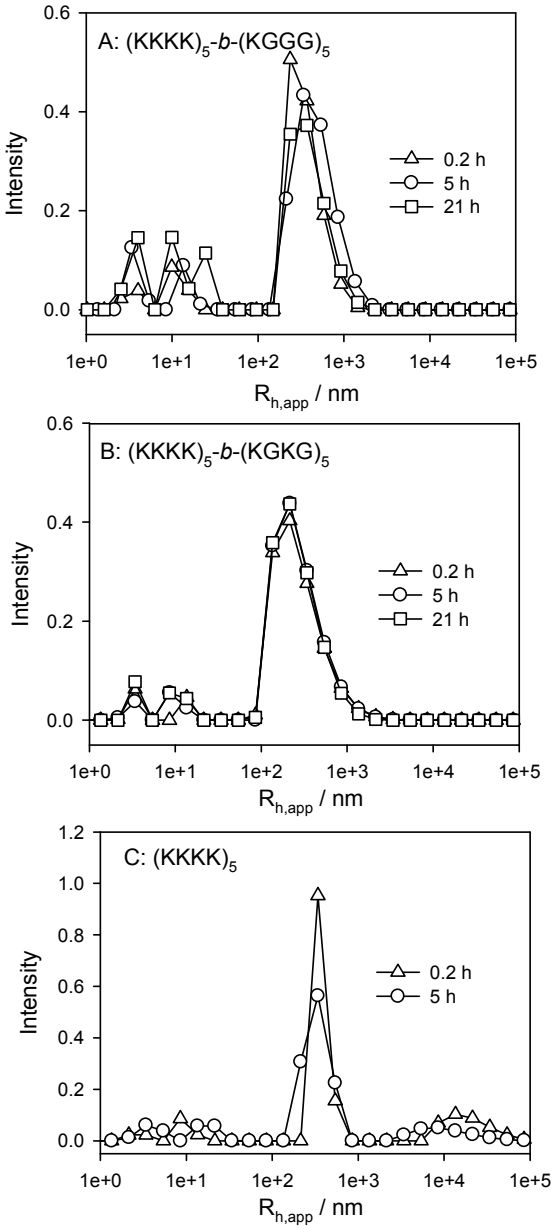

Figure 5. The size distribution of the complexes formed by DNA oligonucleotide and peptide $(KKKK)_5$ (A), $(KKKK)_5$-*b*-$(KGGG)_5$ (B), and $(KKKK)_5$-*b*-$(KGKG)_5$ (C), in the presence of 5% serum. The peaks with size less than 20 nm were derived from serum. *c*(peptide) =1.0×10^{-5} g/mL, *c*(oligonucleotide) = 1.0×10^{-5} g/mL; +/- ratio = 3.0; *c*(serum) = 5%.

To further characterize the surface property of the complexes, their stability in serum was evaluated. Figure 5 shows the $R_{h,app}$ distribution of the complex in the presence of 5% serum over time. When $(KKKK)_5$ peptide solution was mixed with serum, in addition to the complexes, a large cluster over 10 μm was observed. This revealed a further aggregation of the complexes in serum, which progressed over time and visible precipitates were observed in 5 hrs. The decrease in the excess scattered intensity (Figure 6) confirmed the formation of the precipitates at very early stage. Appearance of huge cluster and drop of scattered intensity over a time course were typical features of a

precipitation process.[47] In contrast, the complexes formed by di-block peptides were quite stable in serum. As shown in Figure 5B and 5C, size distribution of these complexes remained nearly identical up to 21 hrs. The scattered intensity also showed no prominent changes in the studied time period (Figure 5), especially for the complex of $(KKKK)_5$-*b*-$(KGKG)_5$.

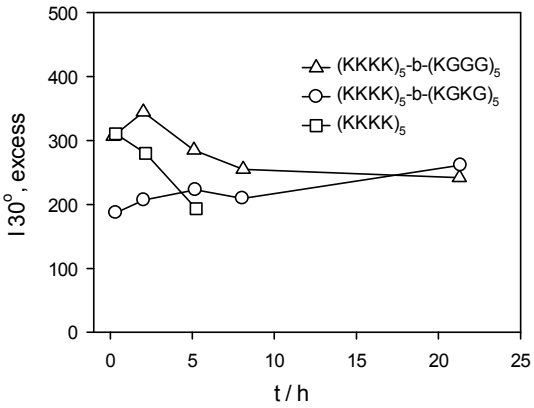

Figure 6. Time dependence of the excess scattered intensity of the complexes in 5% serum. c(peptide) =1.0×10-5 g/mL, c(oligonucleotide) = 1.0×10-5 g/mL; +/- ratio = 3.0.

Cell uptake of complex

The above studies indicated that the complexes formed by DNA oligonucleotide and di-block peptide were different from that of $(KKKK)_5$ peptide. These differences might benefit their bioactivities. To prove this concept, cell uptake assays were performed using HEK293 cells. FITC-labeled oligonucleotide was employed to form complexes with the peptides. Cellular uptake of FITC-labeled oligonucleotide was measured 20 hrs after transfection. Cell uptake efficiency was denoted as the excess fluorescence intensity, in contrast to the naked FITC-DNA sample. Shown in Figure 7, at a +/- ratio of 3.0, cell uptake efficiency was enhanced by 66% and 41% for $(KKKK)_5$-*b*-$(KGKG)_5$ and $(KKKK)_5$-*b*-$(KGGG)_5$, compared to that of the complexes formed by $(KKKK)_5$. To test the performance of the complex at higher charge ratios, the cell uptake efficiencies at a +/- ratio of 9.0 was also studied. Similar results were obtained (Figure S2). The statistical assays together with the confocal microscopy images were included as supporting information.

Even though the zeta potentials of these three complexes were similar, their conformations were different as shown in Figure 4. At current stage, it is difficult to build a relationship between the particle conformation and the cell uptake efficiency. However, the optimal cell uptake efficacy might attribute to the smaller size and higher serum stability of the complexes formed by $(KKKK)_5$-*b*-$(KGKG)_5$ or $(KKKK)_5$-*b*-$(KGGG)_5$, compared to that of $(KKKK)_5$. In addition, the compact structure of the complexes can also protect the siRNA from RNase degradation. Furthermore, the highly-branched conformation revealed in the study might be another beneficial property in complex endocytosis.

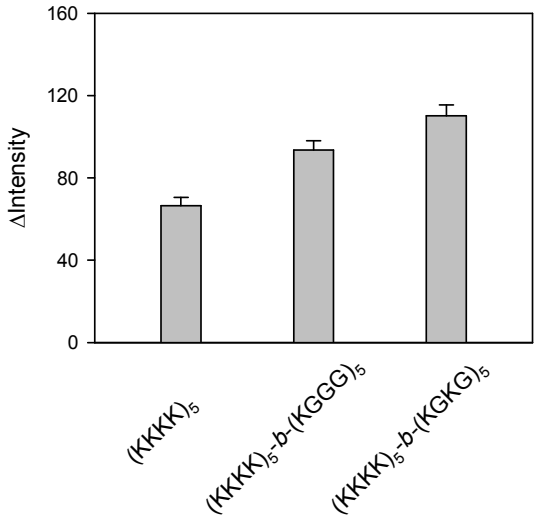

Figure 7. Cell uptake efficiency of peptide/FITC-oligonucleotide complex. Oligonucleotide amount, 100 ng/well, the +/- ratio, 3.0. Data are presented as mean ± SD. Statistic significance are calculated with t-tests. *P value is less than 0.05

Conclusions

Charge density played a essential role in polyelectrolyte complex formation. In general, the polyelectrolyte with a higher charge density dominated the complexation process. Using peptides as model molecules, we demonstrated that the peptide with blocks of different charge density was superior to the peptide of uniform charge density in complex formation. The complexes formed by block peptides and oligonucleotide were shown stable in serum and with improved cell uptake. This probably caused by the weakly charged block, which had the tendency to stay in the periphery of the complex, preventing the complex from further aggregation. The improvement in the structure and selectivity of the complex based on charge density provides more insights for designing non-viral gene delivery vector with high performance.

Peptides provide a platform not only to design polyelectrolyte with precisely-controlled charge density and charge distribution, but also to introduce biofunctions by changing the sequence of amino acids. Since the weakly charged peptides dangle outside the complex, the incorporation of certain sequences aiming at active targeting or endosome escaping should be able to enhance the *in vitro* and *in vivo* transfection activities.

Acknowledgements

This work was supported by the National Natural Science Foundation of China (21174007, 20990232), the Beijing Natural Science Foundation (5132015), the National High-tech

R&D Program of China (2014AA021103, 2012AA022501), the National Basic Research Program of China (2011CBA01102), and the Jianghai Talent Project.

Notes and references

Beijing National Laboratory for Molecular Sciences and the Key Laboratory of Polymer Chemistry and Physics of Ministry of Education, College of Chemistry and Molecular Engineering; State Key Laboratory of Natural and Biomimetic Drugs, School of Pharmaceutical Sciences; Peking University, Beijing 100871, China.
*Email: dliang@pku.edu.cn or quan.du@pku.edu.cn.
‡ Equal contribution

† Footnotes should appear here. These might include comments relevant to but not central to the matter under discussion, limit.ed experimental and spectral data, and crystallographic data.
Electronic Supplementary Information (ESI) available: [Effective charge of the peptides, Confocal microscopy images of cell uptake]. See DOI: 10.1039/b00000

(1) Herweijer, H.; Wolff, J. A. *Gene. Ther.* **2003**, *10*, 453.
(2) Kutzler, M. A.; Weiner, D. B. *Nat. Rev. Genet.* **2008**, *9*, 776.
(3) Wiethoff, C. M.; Middaugh, C. R. *J. Pharm. Sci.* **2003**, *92*, 203.
(4) Castanotto, D.; Rossi, J. J. In *Nature* 2009; Vol. 457, p 426.
(5) Whitehead, K. A.; Langer, R.; Anderson, D. G. *Nat. Rev. Drug. Discov.* **2009**, *8*, 129.
(6) Felgner, P. L.; Gadek, T. R.; Holm, M.; Roman, R.; Chan, H. W.; Wenz, M.; Northrop, J. P.; Ringold, G. M.; Danielsen, M. *P. Natl. Acad. Sci.* **1987**, *84*, 7413.
(7) Lochmann, D.; Jauk, E.; Zimmer, A. *Eur. J. Pharm. Biopharm.* **2004**, *58*, 237.
(8) Li, W. J.; Szoka, F. C. *Pharm. Res.* **2007**, *24*, 438.
(9) Schaffert, D.; Wagner, E. *Gene. Ther.* **2008**, *15*, 1131.
(10) Bae, Y.; Kataoka, K. *Adv. Drug. Deliver. Rev.* **2009**, *61*, 768.
(11) Gao, K.; Huang, L. *Molecular Pharmaceutics* **2009**, *6*, 651.
(12) Mintzer, M. A.; Simanek, E. E. *Chem. Rev.* **2009**, *109*, 259.
(13) Srinivas, R.; Samanta, S.; Chaudhuri, A. *Chem. Soc. Rev.* **2009**, *38*, 3326.
(14) Dautzenberg, H.; Jaeger, W. *Macromol. Chem. Phys.* **2002**, *203*, 2095.
(15) Dai, Z. J.; Wu, C. *Macromolecules* **2012**, *45*, 4346.
(16) Storkle, D.; Duschner, S.; Heimann, N.; Maskos, M.; Schmidt, M. *Macromolecules* **2007**, *40*, 7998.
(17) Dautzenberg, H. *Macromolecules* **1997**, *30*, 7810.
(18) Buchhammer, H. M.; Mende, M.; Oelmann, M. *Colloid Surface A* **2003**, *218*, 151.
(19) Vasilevskaya, V. V.; Leclercq, L.; Boustta, M.; Vert, M.; Khokhlov, R. *Macromolecules* **2007**, *40*, 5934.
(20) Lemmers, M.; Voets, I. K.; Stuart, M. A. C.; van der Gucht, J. *Soft Matter* **2011**, *7*, 1378.
(21) Priftis, D.; Tirrell, M. *Soft Matter* **2012**, *8*, 9396.
(22) Zhou, J. H.; Ke, F. Y.; Xia, Y. Q.; Sun, J. B.; Xu, N.; Li, Z. C.; Liang, D. H. *Polymer* **2013**, *54*, 2521.
(23) Zhou, J. H.; Liu, J.; Shi, T.; Xia, Y. Q.; Luo, Y.; Liang, D. H. *Soft Matter* **2013**, *9*, 2262.
(24) Chu, B. Laser Light Scattering, Basic Principles and Practice, 2nd ed. Academic press. Inc. **1991**.
(25) Bishop, N. E. *Rev. Med. Virol.* **1997**, *7*, 199.
(26) Cabral, H.; Matsumoto, Y.; Mizuno, K.; Chen, Q.; Murakami, M.; Kimura, M.; Terada, Y.; Kano, M. R.; Miyazono, K.; Uesaka, M.; Nishiyama, N.; Kataoka, K. *Nat. Nanotechnol.* **2011**, *6*, 815.
(27) Canton, I.; Battaglia, G. *Chem. Soc. Rev.* **2012**, *41*, 2718.
(28) Champion, J. A.; Mitragotri, S. *P. Natl. Acad. Sci.* **2006**, *103*, 4930.
(29) Kolhar, P.; Anselmo, A. C.; Gupta, V.; Pant, K.; Prabhakarpandian, B.; Ruoslahti, E.; Mitragotri, S. *P. Natl. Acad. Sci.* **2013**, *110*, 10753.
(30) Patnaik, S.; Arif, M.; Pathak, A.; Singh, N.; Gupta, K. C. *Int. J. Pharmaceut.* **2010**, *385*, 194.
(31) Cao, D. W.; Qin, L. H.; Huang, H.; Feng, M.; Pan, S. R.; Chen, J. H. *Mol. Biosyst.* **2013**, *9*, 3175.
(32) Majoros, I. J.; Myc, A.; Thomas, T.; Mehta, C. B.; Baker, J. R. *Biomacromolecules* **2006**, *7*, 572.
(33) Doucede, L.; Migueliz, I.; Arnaiz, E.; Gomez, R.; de la Mata, F. J.; Navarro, G.; de Ilarduya, C. T. *Hum. Gene. Ther.* **2009**, *20*, 1051.
(34) Mita, K.; Zama, M.; Ichimura, S. *Biopolymers* **1977**, *16*, 1993.
(35) Trukhanova, E. S.; Izumrudov, V. A.; Litmanovich, A. A.; Zelikin, A. N. *Biomacromolecules* **2005**, *6*, 3198.
(36) Gref, R.; Domb, A.; Quellec, P.; Blunk, T.; Muller, R. H.; Verbavatz, J. M.; Langer, R. *Adv. Drug. Deliver. Rev.* **1995**, *16*, 215.
(37) Keefe, A. J.; Jiang, S. Y. *Nat. Chem.* **2012**, *4*, 60.
(38) Nowinski, A. K.; White, A. D.; Keefe, A. J.; Jiang, S. Y. *Langmuir* **2014**, *30*, 1864.
(39) Ahmad, A.; Evans, H. M.; Ewert, K.; George, C. X.; Samuel, C. E.; Safinya, C. R. *J. Gene. Med.* **2005**, *7*, 739.
(40) Zhou, J. H.; Wen, H.; Su, C. C.; Niu, L.; Liang, D. H. *Chinese J. Polym. Sci.* **2014**, *32*, 1460.
(41) Schärtl, W. *Springer* **2007**.
(42) Galinsky, G.; Burchard, W. *Macromolecules* **1997**, *30*, 4445.
(43) Trappe, V.; Bauer, J.; Weissmuller, M.; Burchard, W. *Macromolecules* **1997**, *30*, 2365.
(44) Ohshima, H. *Adv. Colloid. Interfac.* **1995**, *62*, 189.
(45) Duval, J. F. L.; Ohshima, H. *Langmuir* **2006**, *22*, 3533.
(46) Fernandez-Nieves, A.; Marquez, M. *J. Chem. Phys.* **2005**, *122*.
(47) Cooper, C. L.; Dubin, P. L.; Kayitmazer, A. B.; Turksen, S. *Curr. Opin. Colloid. In.* **2005**, *10*, 52.